

Models of Toughening of Ceramic/Graphene Composites: a Brief Review

A.G. Sheinerman*

Institute of Problems of Mechanical Engineering, Russian Academy of Sciences, St. Petersburg 199178, Russia

Article history

Received May 20, 2023
Accepted June 01, 2023
Available online June 30, 2023

Abstract

We briefly review the analytical models that describe toughening and fracture toughness reduction in ceramic/graphene composites. We consider such mechanisms of toughening as crack deflection and crack bridging. We examine the effect of pores and fracture along ceramic/graphene interfaces on the fracture toughness reduction at a high graphene volume fraction. The effect of grain boundary sliding on the fracture toughness of ceramic/graphene composites is also considered.

Keywords: Ceramics; Graphene; Composites; Fracture toughness; Cracks

1. INTRODUCTION

The high hardness, wear and corrosion resistance and heat resistance make ceramics excellent materials for tools and bearings [1–4]. However, pure ceramics have low toughness, which makes them prone to fracture [5]. The toughness of ceramics can be increased through the addition of various reinforcing phases [3,4]. In particular, recently, ceramic/graphene composites have attracted much attention. Such composites often exhibit good fracture toughness that can be several times as high as that of similar unreinforced ceramics [6–13].

The high fracture toughness of ceramic/graphene composites is related to the extraordinary properties of graphene [9]. In particular, small volume fractions of platelets of multilayer graphene or reduced graphene oxide can significantly increase the fracture toughness of ceramics, see, e.g., reviews [6–11]. An increase in the fracture toughness of such ceramic/graphene composites is attributed to crack

bridging by graphene inclusions, the pull-out of graphene inclusions from the matrix, crack deflection and branching [14–20], as well as to the presence of graphene wrinkles and out-of-plane compression of graphene platelets [9].

In particular, electron microscopy observations (see, e.g., [9,10,12,16]) of cracks and fracture surfaces of ceramic/graphene composites demonstrate that crack growth is often accompanied by extensive bridging and graphene pull-out. The important role of crack bridging in the toughening of ceramic/graphene composites has also been confirmed by the character of crack resistance curves [7] (where fracture toughness increases with the crack length).

In the present review, we briefly consider theoretical models that describe toughening mechanisms acting in ceramic/graphene composites, as well as the models describing fracture toughness reduction due to grain boundary (GB) sliding, pore formation, or fracture along ceramic/graphene interfaces.

* Corresponding author: A.G. Sheinerman, e-mail: asheinerman@gmail.com

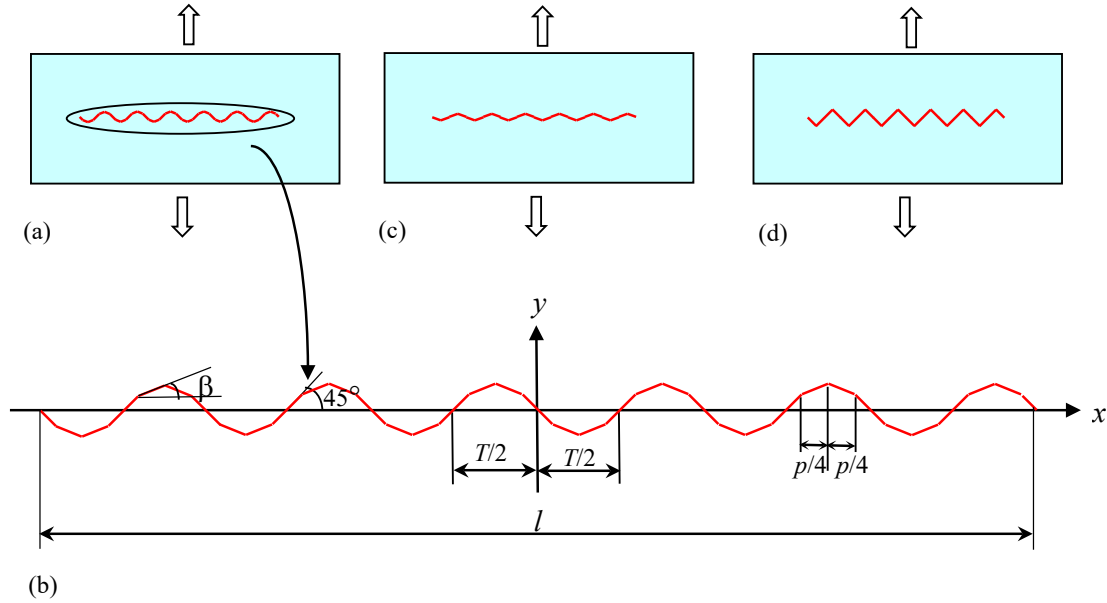


Fig. 1. Geometry of model cracks in the ceramic/graphene composites and pure ceramics under uniaxial tensile loading. (a) Model crack in a ceramic/graphene composite. (b) Geometry of the crack shown in (a). The crack propagates along matrix–graphene interfaces (inclined by $\pm 45^\circ$ with respect to the x -axis) and favorable crystallographic directions in the matrix (inclined by the angle $\pm\beta$ with respect to the x -axis). (c) Model intragrain crack in a ceramic solid. The crack consists of the fragments inclined by the angle $\pm\beta$ with respect to the x -axis. (d) Model grain boundary crack in a polycrystalline or nanocrystalline solid. The crack consists of the fragments inclined by the angle $\pm 30^\circ$ with respect to the x -axis. Reproduced from Ref. [21].

2. MODELS OF TOUGHENING AND FRACTURE TOUGHNESS REDUCTION

First, consider the effect of crack deflection on the fracture toughness of ceramic/graphene composites [21]. The authors of Ref. [21] considered model periodic cracks that approximately describe real cracks that bypass graphene platelets during growth. Using the boundary element method, they calculated the critical stress intensity factor for deflecting mode I cracks, which describes the fracture toughness of the composites containing graphene inclusions. As a reference structure, they examined pure ceramics containing either transgranular or GB cracks. Within model [21], an idealized periodic structure is examined where all graphene platelets have the same dimensions and make the angles of $\pm 45^\circ$ with the normal to the direction of the applied load (Fig. 1a,b). Also, intragrain and GB crack fragments are assumed to make angles $\pm\beta$ with the normal to the direction of the applied load, the distances passed by the crack along all matrix/graphene interfaces are the same, and the distances passed by the crack between neighboring graphene platelets are also the same (Fig. 1). It is also assumed that the crack is periodic with a period T , and its length l is much larger than T (Fig. 1b). The parameter p determines the total distance $p/\cos\beta$ that the crack passes between graphene platelets within each period. In the limiting case of $p = T$, where graphene platelets are absent, the crack transforms to a model periodic intragrain (Fig. 1c) or GB (Fig. 1d) crack in a pure ceramic solid.

The normalized fracture toughness K_{IC}/K_{IC}^0 of a ceramic/graphene composite as a function of graphene volume fraction c calculated under the above assumptions is presented in Fig. 2, for graphene platelet thickness to length ratio of 0.002 and various values of the angle β . Figure 2 demonstrates that graphene platelets increase the fracture toughness of ceramics. The maximum fracture toughness of a composite containing graphene platelets corresponds to the case where the graphene volume fraction c approaches the critical volume fraction c_{cr} at which graphene platelets start to touch each other, producing an easy fracture path. The volume fraction corresponds to the right end points at the curves in Fig. 2. Figure 2 also shows that if cracks in the matrix tend to propagate along GBs, the introduction of an optimum (for toughening) volume fraction of graphene platelets can increase fracture toughness approximately by 50%. At the same time, if cracks in the matrix tend to propagate across grains, the introduction of an optimum volume fraction of graphene platelets can increase fracture toughness by 50–90%, depending on the value of the angle β . Figure 2 also demonstrates that at small graphene volume fraction c , K_{IC} very quickly grows with c , while at larger c , an increase in graphene volume fraction leads only to a slight increase in fracture toughness K_{IC} . Thus, crack deflection in ceramic/graphene composites can increase fracture toughness by up to 50%, if the cracks in the pure ceramics grow along GBs, and by up to 90%, if such cracks tend to be transgranular. These values correlate well with the results of experiments [15–17,22–24] on ceramic/graphene

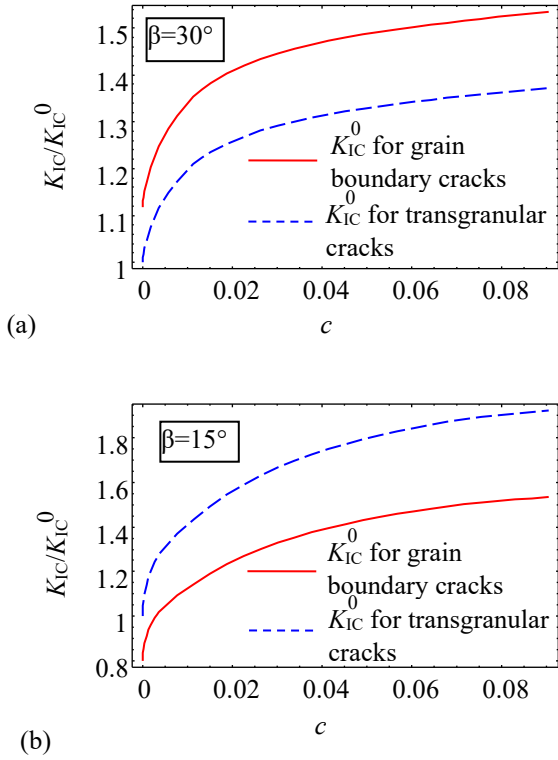


Fig. 2. The ratios of fracture toughness K_{IC} of a ceramic/graphene composite to the fracture toughness K_{IC}^0 of a similar graphene-free ceramic solid as functions of the graphene volume fraction c , for various values of the angle β characterizing the oscillations of the crack direction in the graphene-free ceramic solid. Reproduced from Ref. [21].

composites. Thus, the results in Ref. [21] confirm that crack deflection is an important toughening mechanism that can lead to significant enhancement of the fracture toughness of ceramic/graphene composites.

Now consider the effect of crack bridging on the fracture toughness of ceramic/graphene composites. A model describing this effect has been suggested in Ref. [25]. Within model [25], a straight semi-infinite mode I crack intersects a system of identical platelets (with the equal length and width l and thickness h) perpendicular to the crack plane (Fig. 3). In the region behind the crack tip where the distance between the crack surfaces is smaller than the graphene platelet length l , referred to as the crack-bridging zone, platelets form bridges between the crack surfaces. The friction between the platelets and the ceramic matrix produces the bridging forces, acting at each matrix/platelet interface (Fig. 3). These forces create a resistance to the crack opening, thereby increasing the fracture toughness of the ceramic/graphene composite. In the Cartesian coordinate system (x, y) with the origin at the boundary of the crack-bridging zone (see Fig. 3) these forces (per unit length in the direction normal to the plane of Fig. 3) are written [26] as:

$$f_0(x_i) = \tau(x_i) \left[\frac{l}{2} - v(x_i) \right]. \quad (1)$$

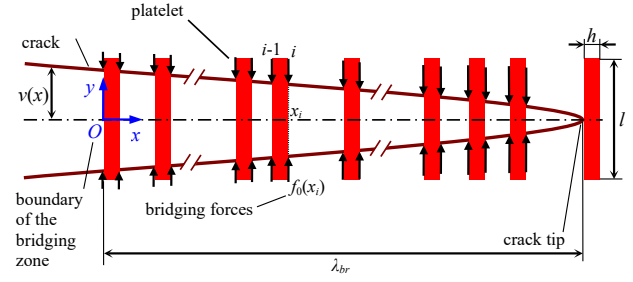


Fig. 3. Crack in a ceramic/graphene composite with aligned graphene platelets. The traction in the crack-bridging zone is discretized into a series of concentrated forces $f_0(x_i)$. Reproduced from Ref. [25].

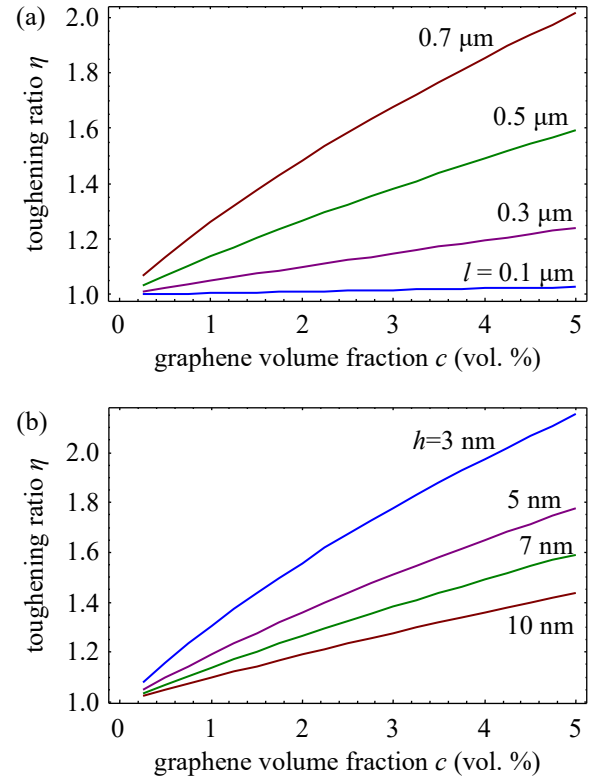


Fig. 4. Dependences of the toughening ratio η on the graphene volume fraction c for YSZ/graphene composites with (a) the graphene platelet thickness $h = 7$ nm and various values of the platelet length l ; (b) the graphene platelet length $l = 0.5$ μm and various values of the platelet thickness h . Reproduced from Ref. [25].

Here x_i are the coordinates of the matrix/platelet interfaces where the forces act (i takes the integers from 1 to N , where N is the total number of bridging forces), $v(x_i)$ is the crack face opening displacement at the position $x = x_i$ (which is equal to the pull-out length of the platelet at the same location), $\tau(x_i)$ is the average shear stress at the interface between the bridging platelet and the matrix. In Ref. [25], it was assumed that for the examined case of ceramic/graphene composites the stress $\tau(x_i)$ does not depend on the crack opening displacement at the point $x = x_i$, so that $\tau(x_i) = \tau_0$, where τ_0 is a material constant.

As a result, the toughening effect of graphene platelets was approximated as being created by a system of bridging forces acting on the crack surfaces. An increase of the fracture toughness due to these bridging forces was calculated numerically by solving a system of on N linear equations for the crack opening displacements. The toughening ratio η (defined as the ratio of fracture toughness of the ceramic/graphene composite to the fracture toughness of a similar graphene-free ceramic solid) calculated in Ref. [25] as a function of the graphene volume fraction c is shown in Fig. 4 for various values of the platelet length l (Fig. 4a) and platelet thickness h (Fig. 4b). The curves in Figs. 4a and 4b are calculated for $h = 7$ nm and $l = 0.5$ μm , respectively. Figure 4 demonstrates that, for a specified graphene volume fraction, the toughening ratio η significantly increases with an increase in the platelet length l and/or a decrease in the platelet thickness h . This implies that for a specified graphene volume fraction, longer platelets produce better crack-bridging-related toughening than smaller ones. Also, the toughening ratio η increases with increasing the graphene content c in the composite, and the normalized increase in fracture toughness due to graphene $(K_{IC} - K_I^0) / K_I^0 = \eta - 1$ scales with the graphene volume fraction c approximately as $\eta - 1 \sim c^{0.8}$. This means that model [25] predicts faster growth of the fracture toughness with the graphene volume fraction than previous models [27,28], which predicted $K_{IC} - K_I^0 \sim c^{1/2}$.

A similar model of crack bridging induced toughening was later suggested in Ref. [29] for the case of SiC/graphene composites. Molecular dynamics (MD) simulations of the platelet pullout during crack opening demonstrated that for SiC/graphene composites, the friction between the matrix and graphene platelet is small, and the bridging forces are mainly related to the formation of free graphene surfaces during graphene pullout from the matrix. As a result, for SiC/graphene composites, the bridging forces (per unit length in the direction normal to the plane of Fig. 3) can be presented as $f_0(x_i) = f_0$, where f_0 is the material constant. In contrast to the case examined in Ref. [25] (see formula (1)), these bridging forces do not depend on the platelet length l or the crack opening displacements $v(x_i)$. The simpler form of the bridging forces $f_0(x_i)$ in Ref. [29] enables one to calculate the fracture toughness of the SiC/graphene composite in a simple analytical form as [30]

$$K_{IC} = \sqrt{t + (K_I^0)^2}, \quad (2)$$

where K_I^0 is the fracture toughness of the composite, which does not account for the bridging effect, $t = (1 + \nu)Gf_0 cl / h$, and G and ν is the shear modulus and Poisson's ratio of the ceramic matrix, respectively. Formula (2) demonstrates that in the model [29] the relative

increase in the fracture toughness $K_{IC} / K_I^0 - 1 = \eta - 1$ scales with the graphene volume fraction c as $\eta - 1 \sim c$ for a small graphene volume fraction (when $t \ll (K_I^0)^2$), and as $\eta - 1 \sim c^{1/2}$ for a high enough graphene volume fraction (when $t \gg (K_I^0)^2$).

The models [25,29] demonstrate that fracture toughness of ceramic/graphene composites should increase with an increase in the graphene platelet length. At the same time, in Ref. [31] it was observed that fracture toughness of alumina/graphene composites decreases with increasing the lateral graphene platelet dimensions. This effect was attributed to the onset of GB sliding in the composites where the length of graphene platelets was close to the GB length. To explain the observed decrease in fracture toughness in alumina/graphene composites, the authors of Ref. [32] suggested a model describing crack propagation assisted by GB sliding in ceramic/graphene composites. Within model [32], graphene platelets in a ceramic/graphene composite can be located both in GBs and in grain interiors and the composite is under uniaxial uniform tension (Fig. 5). Following the observations [31], cracks in the composite are supposed to propagate over GBs. In the framework of model [32], a flat mode I crack, whose length is much larger than the grain size of the ceramic matrix, forms in the composite (Fig. 5a). (Although cracks in the composite are assumed to propagate over GBs, in the latter case, the kinked shape of the crack is neglected, and the crack is approximated as a flat one.) Let the crack terminate at triple junction A (Fig. 5a) and the applied load cause the stress intensity factor K_I near the crack tip. Within model [32], the resolved shear stress, created by the applied load and concentrated at the crack tip, induces sliding over GB AB (Fig. 5b). In turn, GB sliding is carried by edge GB dislocations emitted from triple junction A along GB AB (Fig. 5b). Since GB sliding is retarded near triple junction B, GB dislocations that carry GB sliding are accumulated near this triple junction. The dislocation pile-up at GB AB can lead to the generation and growth of a nano- or microcrack at adjacent GB BC (Fig. 5c). If the stresses, created by the dislocations and the applied load near the crack tip, are high enough, this nano-/microcrack can propagate over entire GB BC (Fig. 5c). Following computer simulations [33–35] and experimental observations [36] of crack propagation in nanomaterials, it is postulated that the formation of nano-/microcrack BC is followed by the crack propagation over GB AB, which results in the coalescence of the large main crack with the new nano-/microcrack (Fig. 5d).

Within model [32], further crack propagation occurs as follows. If a GB adjacent to the crack tip is favorable for crack propagation, that is, makes a relatively small angle with the normal to the loading direction, the crack advances over this GB (Fig. 5e). If all the GBs adjacent to

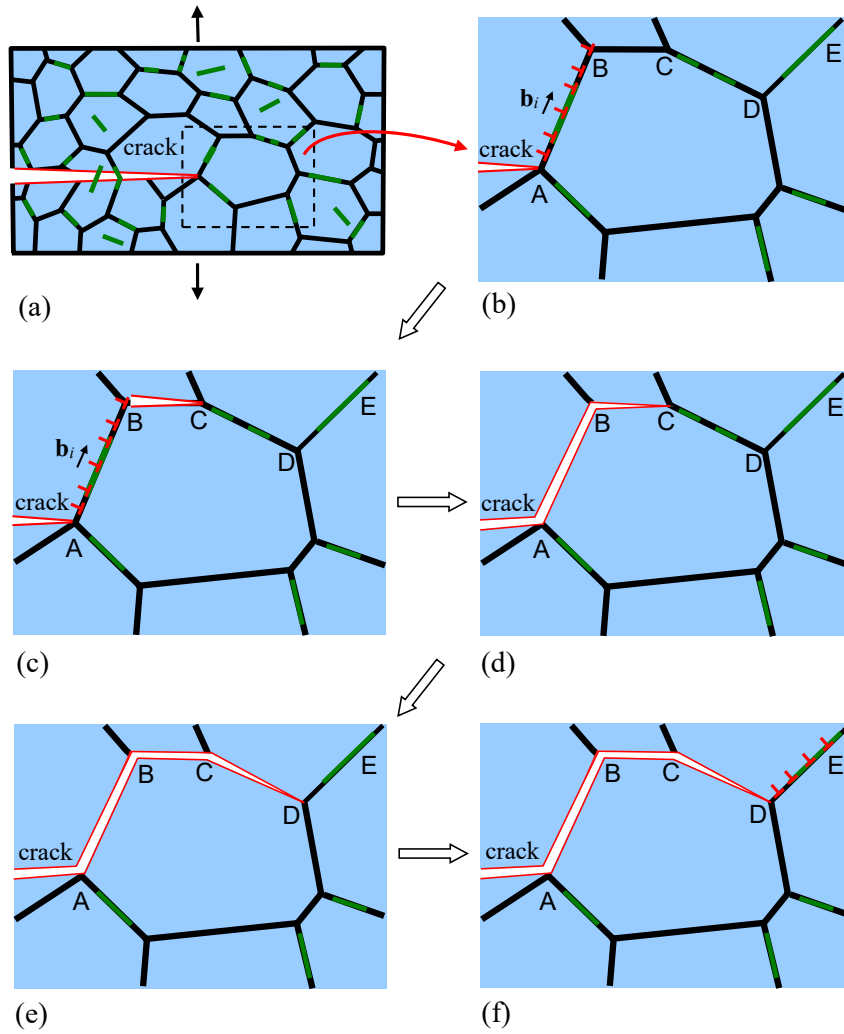


Fig. 5. GB-sliding-assisted crack propagation in ceramic/graphene composites. (a) Model ceramic/graphene composite containing a flat mode I crack. Green lines depict graphene platelets. (b)–(e) Magnified fragments of figure (a) illustrate crack propagation over GBs assisted by GB sliding. (b) Under the action of the stress field induced by the applied tensile load near crack tip A, sliding occurs over GB AB. (c) Dislocations accumulated near triple junction B due to sliding over GB AB induce the generation of a nano- or microcrack in GB BC. (d) The initial main crack and the nano-/microcrack BC merge. (e) Crack propagates over GB CD. (f) Stress concentration near triple junction D induces sliding over GB DE. Reproduced with permission from Ref. [32], © 2019 Elsevier.

the crack tips are not favorable for crack propagation (that is, make large enough angles with the normal to the loading direction), GB sliding occurs over one of these GBs (Fig. 5f), followed by the formation of a new crack at a neighboring GB and its coalescence with the main crack.

The authors of Ref. [32] calculated the critical stress intensity factor characterizing the stresses near the tip of the large crack at which the secondary crack forms and advances over entire GB BC. In the case where the formation and growth of this secondary crack controls the propagation of the pre-existent large crack, this critical stress intensity factor can be considered as the fracture toughness of the ceramic/grapheme composite.

Figure 6a illustrates the dependences of the fracture toughness K_{IC}^{sl} on the normalized graphene platelet length p_1/d_{GB} , for alumina/graphene composites with various values of the GB length d_{GB} . As is seen from Fig. 6a, K_{IC}^{sl}

increases with an increase in the GB length d_{GB} and/or decreasing the length p_1 of graphene platelets. For a specified grain size, an increase of the graphene platelet length p_1 from zero to the GB length d_{GB} can reduce the value of K_{IC}^{sl} by 10–20%.

Figure 6b demonstrates the contour maps of K_{IC}^{sl} in the coordinates $(p_1/d_{GB}, d_{GB})$, for alumina/graphene composites. It is seen that to achieve the fracture toughness of $4.8 \text{ MPa} \times \text{m}^{1/2}$ (which means 50% fracture toughness enhancement compared to pure alumina), the GB length should exceed $2\text{--}7 \mu\text{m}$ (depending on the lateral dimensions of graphene platelets), which corresponds to the grain size exceeding $3\text{--}12 \mu\text{m}$. To achieve the fracture toughness of $4.3 \text{ MPa} \times \text{m}^{1/2}$ (which implies 35% fracture toughness enhancement compared to pure alumina), the GB length should exceed $1\text{--}4 \mu\text{m}$, which corresponds to the grain size exceeding to $2\text{--}7 \mu\text{m}$. Certainly, this is only

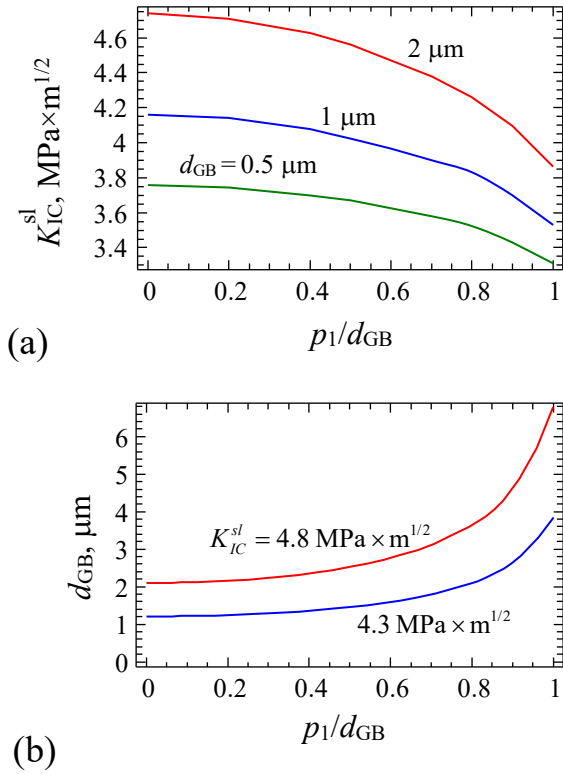


Fig. 6. (a) Fracture toughness K_{IC}^{sl} of an alumina/grapheme composite vs the normalized graphene platelet length p_1/d_{GB} , for various values of the GB length d_{GB} . (b) Contour maps of the fracture toughness K_{IC}^{sl} in the coordinates $(p_1/d_{GB}, d_{GB})$. Reproduced with permission from Ref. [32], © 2019 Elsevier.

the necessary condition for obtaining tough ceramic/graphene composites, which does not guarantee that toughness will be sufficiently improved; to reach this result, the action of such toughening mechanism as crack bridging, graphene platelet pullout, crack deflection or branching is necessary as well.

Although the above toughening mechanisms can increase the toughness of ceramic/grapheme composites, at a high concentration of graphene, the fracture toughness of ceramics decreases with an increase in the volume fraction of graphene [3,6,8,37–39]. In this case, experimental data [3,6,8,37–39] indicate a sharp drop in fracture toughness near a certain critical value of the graphene volume fraction. A sharp decrease in the fracture toughness of ceramic composites with graphene can be associated [37,38] with the agglomeration of graphene platelets and the formation of pores around the formed agglomerates. In Ref. [40], a model was developed that describes the effect of agglomeration of graphene platelets on the fracture toughness of ceramic/grapheme composites.

Within model [40], the agglomeration of graphene platelets occurs during hot pressing of ceramic composites with graphene as a result of graphene sliding along GBs at pressing temperatures. The agglomeration of graphene

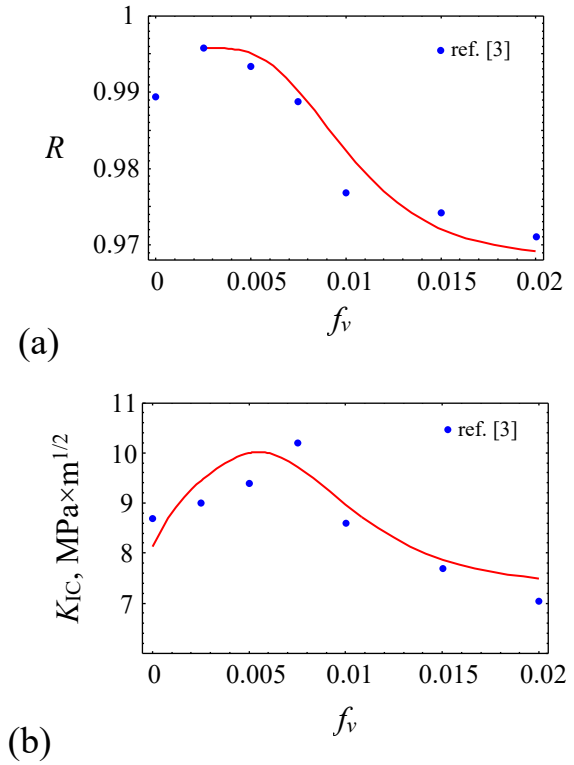


Fig. 7. Dependences of the relative density R (a) and fracture toughness K_{IC} (b) of the Al_2O_3 -WC-TiC-Gr composite on the volume fraction f_v of graphene. For comparison, the blue dots show the experimental values of relative density and fracture toughness [3]. Reproduced with permission from Ref. [40], © 2021 Pleiades Publishing.

platelets during hot pressing occurs if the distance between the centers of these platelets is less than a certain critical value. Taking into account the experimental observations of pores near the agglomerates of graphene platelets [3,6,37,39], the pores are assumed to form near all agglomerates consisting of any greater than one number of graphene platelets.

Under these assumptions, the authors of Ref. [40] calculated the porosity of ceramic/grapheme composites, associated with the agglomeration of graphene platelets, and the relative (dimensionless) density of such composites (defined as the ratio of the actual density of the composite to the density of a similar composite without pores). The dependence of the relative density of the ceramic/grapheme composite on the volume fraction of graphene is shown in Fig. 7a. For comparison, the blue dots in Fig. 7a show the experimental values [3] of the relative density for the Al_2O_3 -WC-TiC composites reinforced with graphene platelets (hereinafter referred to as Al_2O_3 -WC-TiC-Gr). As seen in Fig. 7a, the calculated values of the relative density are in good agreement with experimental data [3].

Following [40], we calculate the effect of pores formed as a result of agglomeration of graphene platelets on the fracture toughness of ceramic/grapheme composites. For

definiteness, assume that the main mechanism for increasing the fracture toughness associated with graphene is crack bridging. In the presence of pores, only platelets that have not undergone agglomeration and, accordingly, are not surrounded by pores contribute to the increase in fracture toughness. In addition, the presence of porosity leads to an additional decrease in the fracture toughness of the material. In the first approximation, to estimate the effect of pores on fracture toughness, we use the results of model [41], which describes the fracture toughness of a material with a rectangular ensemble of cylindrical pores.

The dependence of the fracture toughness K_{IC} of the $\text{Al}_2\text{O}_3\text{-WC-TiC-Gr}$ ceramic composite on the volume fraction f_v of graphene is shown in Fig. 7b. The blue dots in Fig. 7b show the experimental values of fracture toughness [3]. As follows from Fig. 7b, the fracture toughness of the composite first increases and then decreases with increasing volume fraction of graphene. An increase in fracture toughness upon addition of graphene in the interval $f_v < 0.005$ is associated with both a decrease in porosity and the bridging effect. At $f_v > 0.005$, pores begin to form in the material near the graphene platelets, and the bridging effect gradually disappears, while the negative effect of pores on fracture toughness increases. As seen in Fig. 7b, the calculated curve agrees satisfactorily with the experimental values [3] of the fracture toughness of the $\text{Al}_2\text{O}_3\text{-WC-TiC-Gr}$ ceramic composite.

Thus, model [40] explains the observed (for example, [3,6,8,37–39]) drop in the fracture toughness of ceramic/graphene composites when the volume fraction of graphene exceeds a critical value. It is shown that the deterioration of the fracture toughness can be associated with the formation of pores around the agglomerates of graphene platelets.

At the same time, a drop in fracture toughness of ceramic/graphene composites above some critical volume fraction of graphene has been observed [42] even in fully dense ceramic/graphene composites. A model that describes fracture toughness reduction due to such interfaces was suggested in Ref. [30].

Model [30] focuses on the situation where graphene platelets are located at GBs and the length of graphene platelets is, on average, at least, several times larger than the length of GBs. In this situation, one can neglect the relatively small number of GBs partially occupied by graphene and treat all GBs as being either graphene-free or entirely occupied by graphene. Within model [30] the principle toughening mechanism of the composite associated with the presence of graphene platelets is crack bridging by graphene platelets, and the toughening due to crack bridging is described by formula (2).

It is also assumed that the ceramic/graphene interfaces are weaker than the GBs of the ceramic matrix.

This means that the ceramic/graphene adhesive energy (the specific energy required to tear graphene platelets from the ceramic matrix) is smaller than the specific energy required for the fracture at graphene-free GBs. In this situation, the presence of graphene at GBs can promote the fracture of individual GBs, thereby decreasing fracture toughness at high graphene content. As a result, the total effect of graphene on fracture toughness is determined by the balance of crack bridging (that toughens the composite) and interface weakening (that reduces fracture toughness).

Within [30], the specific energies that characterize the fracture of graphene-free GBs and GBs containing graphene platelets lie in some intervals, and the GBs adjacent to the tip of a pre-existent crack are characterized by a probability of fracture. As a first approximation, to analyze crack propagation across GBs near the crack tip, the author of Ref. [30] exploited the results obtained for bond percolation in a two-dimensional hexagonal lattice. Within such an approach, the crack can grow catastrophically if the probability of fracture of GBs adjacent to the crack tip exceeds some critical value. As a result, the fracture toughness that accounts both the effects of crack bridging and fracture along weak ceramic/graphene interfaces was calculated.

The dependences of the corresponding fracture toughness \bar{K}_{IC} of an $\alpha\text{-Al}_2\text{O}_3$ /graphene composite on the GB fraction f occupied by graphene are presented in Fig. 8, for two different values of the ratio L/d of the graphene platelet length L and GB length d . It follows from Fig. 8 that fracture toughness increases with f until the value of f becomes close to the percolation threshold $f = 0.6527$. After that fracture toughness rapidly decreases due to crack percolation over graphene platelets. The maximum value of \bar{K}_{IC} increases with L/d .

Thus, Figure 8 predicts that even in fully dense ceramic/graphene composites, there is an optimum graphene

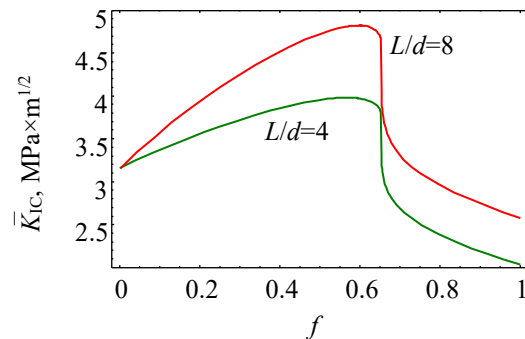


Fig. 8. Evolution of the fracture toughness \bar{K}_{IC} of $\alpha\text{-Al}_2\text{O}_3$ /graphene composite with the fraction f of grain boundaries occupied by graphene, for various values of normalized graphene platelet length L/d . Reproduced with permission from Ref. [30], © 2023 Elsevier.

volume fraction that corresponds to the maximum fracture toughness of ceramic/graphene composites. Above this volume fraction, fracture toughness decreases with an increase in the graphene content. The calculated dependences in Fig. 8 explain the experimental observations [42] of the fracture toughness reduction above certain graphene content in fully dense ceramic/graphene composites.

3. SUMMARY

In summary, from the above brief review it follows that crack bridging and crack deflection are the important toughening mechanisms in ceramic/graphene composites that can dramatically increase their fracture toughness. At the same time, at high enough volume fraction of graphene the fracture toughness of such composites drops due to the formation of voids around or near graphene agglomerates and/or the fracture along ceramic/graphene interfaces. The optimum toughening can be achieved by using long graphene platelets, whose lateral dimensions in the case of fine-grained ceramic matrix is not too close to the typical length of grain boundaries.

REFERENCES

- [1] Y. Cheng, Y. Zhang, T. Wan, Z. Yin, J. Wang, *Mechanical properties and toughening mechanisms of graphene platelets reinforced Al₂O₃/TiC composite ceramic tool materials by microwave sintering*, Mater. Sci. Eng. A, 2017, vol. 680, pp. 190–196.
- [2] P.C. Milak, F.D. Minatto, A. De Noni Jr., O.R.K. Montedo, *Wear performance of alumina-based ceramics - a review of the influence of microstructure on erosive wear*, Cerâmica, 2015, vol. 61, pp. 88–103.
- [3] X. Wang, J. Zhao, E. Cui, S. Song, H. Liu, W. Song, *Microstructure, mechanical properties and toughening mechanisms of graphene reinforced Al₂O₃-WC-TiC composite ceramic tool material*, Ceram. Int., 2019, vol. 45, no. 8, pp. 10321–10329.
- [4] F. Chen, K. Yan, X. Zhang, Y. Zhu, J. Hong, *Microscale simulation method for prediction of mechanical properties and composition design of multilayer graphene-reinforced ceramic bearings*, Ceram. Int., 2021, vol. 47, no. 12, pp. 17531–17539.
- [5] W. Kim, H.S. Oh, I.J. Shon, *The effects of graphene reinforcement on the mechanical properties of Al₂O₃ ceramics rapidly sintered by high-frequency induction heating*, Int. J. Refract. Metals Hard Mater., 2015, vol. 48, pp. 376–381.
- [6] H. Porwal, S. Grasso, M.J. Reece, *Review of graphene-ceramic matrix composites*, Adv. Appl. Cer., 2013, vol. 112, no. 8, pp. 443–454.
- [7] A. Centeno, V.G. Rocha, B. Alonso, A. Fernandez, C.F. Gutierrez-Gonzalez, R. Torrecillas, A. Zurutuza, *Graphene for tough and electroconductive alumina ceramics*, J. Eur. Ceram. Soc., 2013, vol. 33, no. 15–16, pp. 3201–3210.
- [8] A. Nieto, A. Bisht, D. Lahiri, C. Zhang, A. Agarwal, *Graphene reinforced metal and ceramic matrix composites: a review*, Int. Mater. Rev., 2017, vol. 62, no. 5, pp. 241–302.
- [9] P. Miranzo, M. Belmonte, M.I. Osendi, *From bulk to cellular structures: A review on ceramic/graphene filler composites*, J. Eur. Ceram. Soc., 2017, vol. 37, no. 12, pp. 3649–3672.
- [10] I.A. Ovid'ko, *Micromechanics of fracturing in nanoceramics*, Philos. Trans. R. Soc. A, 2015, vol. 373, no. 2038, art. no. 20140129.
- [11] A.G. Glukharev, V.G. Konakov, *Synthesis and properties of zirconia-graphene composite ceramics: a brief review*, Rev. Adv. Mater. Sci., 2018, vol. 56, no. 1, pp. 124–138.
- [12] Q. Wang, C. Ramirez, C.S. Watts, O. Borrero-López, A.L. Ortiz, B.W. Sheldon, N.P. Padture, *Fracture, fatigue, and sliding-wear behavior of nanocomposites of alumina and reduced graphene-oxide*, Acta Mater., 2020, vol. 186, pp. 29–39.
- [13] C. Sun, Y. Huang, Q. Shen, W. Wang, W. Pan, P. Zong, L. Yang, Y. Xing, C. Wan, *Embedding two-dimensional graphene array in ceramic matrix*, Sci. Adv., 2020, vol. 6, no. 39, art. no. eabb1338.
- [14] L.S. Walker, V.R. Marroto, M.A. Rafice, N. Koratkar, E.L. Corral, *Toughening in graphene ceramic composites*, ACS Nano, 2011, vol. 5, no. 4, pp. 3182–3190.
- [15] O. Tapasztó, L. Tapasztó, M. Markó, F. Kern, R. Gadow, C. Balázi, *Dispersion patterns of graphene and carbon nanotubes in ceramic matrix composites*, Chem. Phys. Lett., 2011, vol. 511, no. 4–6, pp. 340–343.
- [16] K. Wang, Y. Wang, Z. Fan, J. Yan, T. Wei, *Preparation of graphene nanosheet/alumina composites by spark plasma sintering*, Mater. Res. Bull., 2011, vol. 46, pp. 315–318.
- [17] L. Kvetková, A. Duszová, P. Hvizdoš, J. Dusza, P. Kun, C. Balázi, *Fracture toughness and toughening mechanisms in graphene platelet reinforced Si₃N₄ composites*, Scr. Mater., 2012, vol. 66, no. 10, pp. 793–796.
- [18] J. Liu, H. Yan, J. Reece, K. Jiang, *Toughening of zirconia/alumina composites by the addition of graphene platelets*, J. Eur. Ceram. Soc., 2012, vol. 32, no. 16, pp. 4185–4193.
- [19] A. Nieto, D. Lahiri, A. Agarwal, *Graphene nanoplatelets reinforced tantalum carbide consolidated by spark plasma sintering*, Mater. Sci. Eng. A, 2013, vol. 582, pp. 338–346.
- [20] H. Porwal, P. Tatarko, S. Grasso, J. Khaliq, I. Dlouhý, M.J. Reece, *Graphene reinforced alumina nanocomposites*, Carbon, 2013, vol. 64, pp. 359–369.
- [21] I.A. Ovid'ko, A.G. Sheinerman, *Toughening due to crack deflection in ceramic- and metal-graphene nanocomposites*, Rev. Adv. Mater. Sci., 2015, vol. 43, no. 1/2, pp. 52–60.
- [22] K. Chu, C. Jia, *Enhanced strength in bulk graphene-copper composites*, Phys. Status Solidi A, 2014, vol. 211, no. 1, pp. 184–190.
- [23] T. He, J. Li, L. Wang, J. Zhu, W. Jiang, *Preparation and consolidation of alumina/graphene composite powders*, Mater. Trans., 2009, vol. 50, no. 4, pp. 749–751.
- [24] J. Lui, H. Yan, K. Jiang, *Mechanical properties of graphene platelet-reinforced alumina ceramic composites*, Ceram. Int., 2013, vol. 39, no. 5, pp. 6215–6221.
- [25] S.V. Bobylev, A.G. Sheinerman, *Effect of crack bridging on the toughening of ceramic/graphene composites*, Rev. Adv. Mater. Sci., 2018, vol. 57, no. 1, pp. 54–62.
- [26] Y. Shao, H.-P. Zhao, X.-Q. Feng, H. Gao, *Discontinuous crack-bridging model for fracture toughness analysis of nacre*, J. Mech. Phys. Solids, 2012, vol. 60, no. 8, pp. 1400–1419.

- [27] C. Ramirez, M.I. Osendi, *Toughening in ceramics containing graphene fillers*, *Ceram. Int.*, 2014, vol. 40, no. 7B, pp. 11187–11192.
- [28] L. Zhang, X.G. Zhang, Y. Chen, J.N. Su, W.W. Liu, T.H. Zhang, Y.T. Wang, *Interfacial stress transfer in a graphene nanosheet toughened hydroxyapatite composite*, *Appl. Phys. Lett.*, 2014, vol. 105, no. 16, art. no. 161908.
- [29] Y.C. Wang, Y.B. Zhu, Z.Z. He, H.A. Wu, *Multiscale investigations into the fracture toughness of SiC/graphene composites: Atomistic simulations and crack-bridging model*, *Ceram. Int.*, 2020, vol. 46, no. 18A, pp. 29101–29110.
- [30] A.G. Sheinerman, *Modeling of fracture toughness enhancement and reduction in fully dense ceramic/graphene composites*, *Eur. J. Mech. A*, 2023, vol. 98, art. no. 104891.
- [31] H. Porwal, R. Sagar, P. Tatarko, S. Grasso, T. Saunders, I. Dlouhý, M.J. Reece, *Effect of lateral size of graphene nano-sheets on the mechanical properties and machinability of alumina nano-composites*, *Ceram. Int.*, 2016, vol. 42, no. 6, pp. 7533–7542.
- [32] A.G. Sheinerman, N.F. Morozov, M.Yu. Gutkin, *Effect of grain boundary sliding on fracture toughness of ceramic/graphene composites*, *Mech. Mater.*, 2019, vol. 137, art. no. 103126.
- [33] D. Farkas, H. Van Swygenhoven, P.M. Derlet, *Intergranular fracture in nanocrystalline metals*, *Phys. Rev. B*, 2002, vol. 66, no. 6, art. 060101(R).
- [34] H. Van Swygenhoven, P.M. Derlet, A. Hasnaoui, M. Samaras, *Impact of grain boundaries on structural and mechanical properties*, in: *Nanostructures: synthesis, functional properties and applications*, ed. by T. Tsakalakos, I.A. Ovid'ko, A.K. Vasudevan, Springer, Dordrecht, 2003, pp. 155–167.
- [35] A. Latapie, D. Farkas, *Molecular dynamics investigation of the fracture behavior of nanocrystalline α -Fe*, *Phys. Rev. B*, 2004, vol. 69, no. 13, art. no. 134110.
- [36] E. Hosseinian, S. Gupta, O.N. Pierron, M. Legros, *Size effects on intergranular crack growth mechanisms in ultrathin nanocrystalline gold free-standing films*, *Acta Mater.*, 2018, vol. 143, pp. 77–87.
- [37] K. Markadan, J.K. Chin, M.T.T. Tan, *Recent progress in graphene based ceramic composites: a review*, *J. Mater. Res.*, 2017, vol. 32, no. 1, pp. 84–106.
- [38] K.I. Vishnu Vandana, K.N.S. Suman, *Hardness and fracture toughness of ceramic composite using experimental and analytical methods*, *Int. J. Eng. Adv. Technol.*, 2019, vol. 9, no. 2, pp. 5250–5254.
- [39] C. Ramirez, P. Miranzo, M. Belmonte, M.I. Osendi, P. Poza, S.M. Vega-Diaz, M. Terronez, *Extraordinary toughening enhancement and flexural strength in Si_3N_4 composites using graphene sheets*, *J. Eur. Ceram. Soc.*, 2014, vol. 34, no. 2, pp. 161–169.
- [40] A.G. Sheinerman, S.A. Krasnitskii, *Modeling of the influence of graphene agglomeration on the mechanical properties of ceramic composites with graphene*, *Tech. Phys. Lett.*, 2021, vol. 47, no. 12, pp. 873–876.
- [41] M. Liu, C. Chen, *A micromechanical analysis of the fracture properties of saturated porous media*, *Int. J. Solids Struct.*, 2015, vol. 63, pp. 32–38.
- [42] E. Bódis, I. Cora, C. Balázs, P. Németh, Z. Károly, S. Klébert, P. Fazekas, A.M. Keszler, J. Szépvölgyi, *Spark plasma sintering of graphene reinforced silicon carbide ceramics*, *Ceram. Int.*, 2017, vol. 43, no. 12, pp. 9005–9011.

УДК 539.422.5+539.421

Модели повышения вязкости разрушения композитов «керамика/графен»: краткий обзор

А.Г. Шейнерман

Институт проблем машиноведения РАН, Санкт-Петербург 199178, Россия

Аннотация. Кратко рассмотрены аналитические модели, описывающие увеличение и снижение вязкости разрушения композитов «керамика/графен». Рассмотрены такие механизмы упрочнения, как искривление трещин и образование мостиков между их берегами. Исследовано влияние пор и разрушения вдоль границ раздела «керамика/графен» на уменьшение вязкости разрушения при высокой объемной доле графена. Также рассмотрено влияние межзеренного скольжения на вязкость разрушения композитов «керамика/графен».

Ключевые слова: керамика; графен; композиты; вязкость разрушения; трещины